

Quantum and stringy corrections to the equation of state of holographic QCD matter and the nature of the chiral transition

T. Alho^a, M. Järvinen^b, K. Kajantie^c, E. Kiritsis^{d,e}, K. Tuominen^c

^a*University of Iceland, Science Institute, Dunhaga 3, 107 Reykjavik, Iceland*

^b*Laboratoire de Physique Théorique, École Normale Supérieure and Institut de Physique Théorique Philippe Meyer, 24 rue Lhomond, 75231 Paris Cedex 05, France*

^c*Helsinki Institute of Physics, P.O.Box 64, FI-00014 University of Helsinki, Finland*

^d*Crete Center for Theoretical Physics, Department of Physics, University of Crete, 71003 Heraklion, Greece.*

^e*Univ Paris Diderot, Sorbonne Paris Cité, APC, UMR 7164 CNRS, F-75205 Paris, France.*

We consider the finite temperature phase diagram of holographic QCD in the Veneziano limit ($N_c \rightarrow \infty$, $N_f \rightarrow \infty$ with $x_f = N_f/N_c$ fixed) and calculate one string-loop corrections to the free energy in certain approximations. Such corrections, especially due to the pion modes are unsuppressed in the Veneziano limit. We find that under some extra assumptions the first order transition following from classical gravity solutions can become second order. If stringy asymptotics are of a special form and there are residual interactions it may even become of third order. Operationally these computations imply modelling the low temperature chiral symmetry breaking phase with a hadron gas containing N_f^2 massless Goldstone bosons and an exponential spectrum of massive hadrons. A third order transition is possible only if repulsive hadron interactions via the excluded volume effect are included.

Contents

1	Introduction	1
2	The pressure in high and low temperature phases	4
2.1	High temperature pressure and vacuum spectrum from a holographic model .	4
2.2	The pressure at low temperature modelled as a hadron gas	7
3	Connecting hadron gas with plasma	9
3.1	Second order transition	10
3.2	Third order transition with pointlike mesons	11
4	Third order transition with excluded volume corrections	12
5	Fit of parameters and their x_f dependence	15
6	Second order transition with massive Goldstone bosons	19
7	Conclusions	19

1 Introduction

In this paper we consider thermodynamics of QCD at finite temperature in a non-critical holographic model [1] and show how one can effectively compute quantum 1-loop and even stringy corrections by phenomenological considerations relating to the hadronic phase. We will then have thermodynamics at all temperatures together with an analysis of possible phase transitions.

Holographic models of QCD (V-QCD) in the Veneziano limit,

$$N_c \rightarrow \infty \quad , \quad N_f \rightarrow \infty \quad , \quad x_f \equiv \frac{N_f}{N_c} \text{ fixed}, \quad (1)$$

have been proposed and studied in [1, 2, 3, 4], based on earlier proposals for pure Yang-Mills [5] and the identification of the chiral condensate as the tachyon of string theory [6]. In such theories for a small enough number of flavours, $x_f < x_c \simeq 4$ the low energy theory is QCD-like: it has chiral symmetry breaking, $N_f^2 - 1$ massless pions (when quarks are massless) and confinement.

The finite temperature study of V-QCD at zero baryon density and for massless quarks, [2] revealed the possibility of one or two possible phase transitions, depending on the asymptotics of scalar potentials:

- (a) One phase transition. In this case the theory at a specific critical temperature T_c jumps to a black hole solution with restored chiral symmetry. The transition is a first order one and is at the same time a deconfinement and a chiral restoration transition.

- (b) Two phase transitions. In this case the theory at a specific critical temperature T_c jumps to a black hole solution which breaks chiral symmetry. The transition is first order and the theory is in a deconfined plasma phase with broken chiral symmetry. At a higher temperature there is a second transition, second order this time, and the system is described by a black hole solution with unbroken chiral symmetry.

The chiral phase transition above can be characterised by a chiral condensate which is an exact order parameter for massless quarks. Although in the presence of quarks there is no order parameter for confinement, at large N_c , one can use the scaling of the free energy F with N_c . A phase in which $F \sim \mathcal{O}(N_c^2)$ is a deconfined phase while a phase where $F \sim \mathcal{O}(1)$ is a confinement phase. In a holographic theory therefore, any phase transition in which the system jumps from the $T = 0$ saddle point (or the “thermal gas solution” as it is known) to a black hole saddle point, is a deconfinement transition.¹

In [3] a finite temperature and finite density study was made for a V-QCD model with two phase transitions (in case (b) above). Since then further analysis has indicated that case (a) above is preferred when generic properties of the mesonic radial trajectories are imposed [10, 11]. This is the version of the theory we will use in this work.

As it was already stressed in [1], holographic theories in the Veneziano limit have more uncontrolled phenomena compared to theories in the standard 't Hooft limit. The reason is that in the open string theory sector where the fundamental degrees of freedom arise (quarks) as endpoints of open strings, the effective coupling constant is $g_s N_f$ where g_s is the closed string coupling $g_s \sim \frac{1}{N_c}$.

In the 't Hooft limit where N_f is kept fixed and of order one, $g_s N_f \sim \frac{1}{N_c}$ and contributions from open string loops are suppressed. This is equivalent to the fact that quark loops are suppressed in the QFT. In the Veneziano limit however, $g_s N_f \sim x_f \sim \mathcal{O}(1)$ and open string loops are unsuppressed. This can be easily checked in a simple one loop diagram that corrects a propagator and pions (or in general non-singlet mesons) go around the loop: the diagram for a single meson is suppressed by $\frac{1}{N_c^2}$ but there are $N_f^2 - 1$ non-singlet mesons going around the loop, bringing back this contribution to become of $\mathcal{O}(1)$.

In this paper we will start an investigation of such corrections. The brute-force method is to compute the one-loop corrections to the free-energy in the dual string theory, something that is in principle possible in string theory [12]. In our case however we are limited by the fact that we do not know the full string theory, and even if known it requires a complete solution at tree level in order for the full one-loop contribution to be computed. For comparison this is not yet known even in the best known case of holography: that of $\mathcal{N} = 4$ super Yang-Mills.

We will have therefore to be more modest, and we will use physical arguments to isolate and compute the most important contributions in the domain $0 < x_f < x_c$ to the free energy of the confined saddle point: the thermal gas solution. The reason is that at tree level the free-energy of the thermal gas solution is $\mathcal{O}(1)$ and therefore is neglected compared to the deconfined free energy that is $\mathcal{O}(N_c^2)$. At one-loop however the correction, being proportional to the meson multiplicities is of $\mathcal{O}(N_f^2)$ and therefore of the same order as the deconfined free energy in the Veneziano limit.

¹Of course this structure of two transitions is not specific to holography, but a similar structure emerges in conventional effective model approaches to QCD matter thermodynamics, see e.g. [7, 8, 9].

The string one-loop calculation to the free energy in the confined phase can be divided into an infinite number of one-loop calculations where each of the string states goes around the loop. It depends only on the quadratic part of the tree level action and not on interactions. If one can diagonalize the tree-level action then the result can be given in terms of one-loop finite temperature diagrams of particles with given tree level masses. For the important meson trajectories and the present holographic theory, this was done in [10, 11].

For practical purposes we will split the non-singlet spectrum of the string theory in question (this is the one that gives the dominant contribution, the singlet spectrum contribution is down by a factor of N_f^{-2}) as follows:

1. The massless sector. This includes the $N_f^2 - 1$ massless pions.
2. The massive meson sector of the four main meson trajectories. This includes the fields generated out of the vacuum by the three important low dimension operators in the meson sector: the quark mass term (massive pseudoscalars and massive scalars), the vector current (massive vector mesons, starting with the ρ) and the axial current (massive axial vector mesons). The masses and widths of these mesons were computed in [10, 11], where it was shown that after the lightest 2-3 mesons the rest of the masses are described by linear radial trajectories of the form $m_n^2 \simeq a n$ with a a universal computable constant.
3. The full string spectrum that includes an infinite number of extra fields. Such fields corresponds to higher spin mesons that appear at higher levels in the string spectrum and therefore the lightest mass of their trajectory is higher than the four basic trajectories. As the detailed string theory spectrum for V-QCD is not known, we will parametrize such a spectrum by a density of states in order to estimate their impact on the thermodynamics.

Concretely, the above is implemented as follows in this holographic setup. To begin with, the free energy $-f = p_q(T, \mu = 0; N_c, N_f, m_q = 0)$ in the QCD plasma phase is computed so that it is normalised to the Stefan-Boltzmann limit at $T \rightarrow \infty$. It is valid for $T_{\min} < T < \infty$, where T_{\min} is the temperature where the gravity solution corresponding to the QCD plasma phase becomes thermodynamically unstable.

The computation of the pressure $p_h(T)$ down to $T = 0$ involves the stages 1-3 outlined above. First, at stage 1 Goldstone bosons with

$$p_{h,\text{id}}(T)/T^4 = \frac{\pi^2}{90} (N_f^2 - 1) \quad (2)$$

are included. They arise as zero modes of the 1-loop computation. Comparing with p_q shows that a 1st order deconfining transition takes place. Second, at stage 2 some states from the lower trajectories are included to give us $p_h(T)$. A numerical analysis shows that they only have a small effect and the transition still remains 1st order. Finally, at stage 3 the entire mass spectrum including lower Regge trajectories and with mesonic interactions is needed.

We shall model this by an exponential Hagedorn mass spectrum [13]-[30], see Eq. (19) below. Effectively, one has a mesonic string model for hadrons; these are less well developed

for baryons but we here address the case of zero net baryon number, $\mu = 0$. The mass spectrum contains a number of parameters, which are strongly constrained by how $p_h(T)$ and $p_q(T)$ connect at T_c . We shall see that in this model it is easy to enforce constancy of both $\hat{p} \equiv p/T^4$ and of its logarithmic T -derivative, the interaction measure $(\epsilon - 3p)/T^4$. The chiral transition would then be of 2nd order. However, the second logarithmic T -derivative thereof would then be discontinuous and the interaction measure would exhibit a sharp peak at T_c .

Our goal is to proceed one step further and demand also the continuity of the second logarithmic derivative. This is actually quite complicated to achieve, as the second logarithmic derivatives are naturally of opposite signs. We find that to change the sign of the second derivative of the hadronic pressure and to accomplish required equality one has to include interactions in the hadron gas phase. It is enough to include repulsive Van der Waals-type interactions caused by the finite size of hadrons. The transition then is of third order (as in 2-dimensional lattice $SU(N \rightarrow \infty)$ gauge theory [31, 32]) and actually the shape of the interaction measure resembles that of a Tracy-Widom distribution [33, 34]. With increasing x_f one sees concretely how the thermodynamics approaches that in the conformal region $x_f > x_c$.

Our analysis does not prove that the transition is of third order, just analyses a possible framework. Universality arguments based on the epsilon expansion [35] indicate a 1st order transition for $N_f \geq 3$ at fixed N_c . In [3] we discuss why this conclusion might not be valid for the case studied here. If the transition is continuous, $p(T)$ is analytic at all T . How the hadronic and plasma phases then should be connected for massive quarks is discussed in [28]. This is excluded in the holographic approach in which the plasma pressure $p_q(T)$ is valid only for $T > T_{\min}$. Notice also that the analysis of QCD in the Veneziano limit by using weak coupling expansion on $S^1 \times S^3$ suggests that the transition is a crossover or of very high order [36] (see also [37]).

One obvious extension of the above is explicit chiral symmetry breaking induced by quark masses. Then the massless Goldstone bosons would entirely disappear.

Section 2 below outlines the numerical computation of $p_q(T)$ from holography [38], and summarizes hadron gas formulas. Section 3 discusses a second order connection and the difficulties of a third order connection. The formalism of including hadronic interactions via the excluded volume correction is presented in Section 4 and results computed from this are presented in Section 5 where also the x_f -dependence of the results is discussed. A simple modelling of what happens if quarks are massive is contained in Section 6.

2 The pressure in high and low temperature phases

2.1 High temperature pressure and vacuum spectrum from a holographic model

To compute the pressure at temperatures above the phase transition, we apply a model for a 5-dimensional gravity dual of QCD matter with large N_c and $N_f = x_f N_c$ originally proposed in [1] and studied in [2] and [3] (thermodynamics) and [11] (mass spectrum). The details of the model have been thoroughly exposed in [2, 3], and here we only briefly recall some of the

general details.

The model builds on asymptotically AdS₅ metric $g_{\mu\nu}$, specified by $ds^2 = b^2(z)(-f(z)dt^2 + d\mathbf{x}^2 + dz^2/f(z))$. In addition to gravity, the model contains bulk scalars, a dilaton $\lambda(z)$, a tachyon $\tau(z)$, and the scalar potential (the zeroth component of the gauge field) $\Phi(z)$. The scalar $1/\lambda$ sources the field theory operator $\text{Tr}F_{\mu\nu}^2$. The vacuum solution $\lambda(z)$ is therefore identified with the gauge theory coupling $N_c g^2(\mu)/(8\pi^2)$.

Furthermore, the dependence of the fields on the coordinate z in this model is constrained to reproduce the renormalisation group flow of the dual gauge theory in the UV (i.e., for $z \rightarrow 0$). For the field λ this means that $1/\lambda(z) \approx b_0 \log(\Lambda z)$ as $z \rightarrow 0$, where $b_0 = \frac{1}{3}(11 - 2N_f)$ is the one-loop coefficient of the beta function². Here we also see that Λ is analogous to the scale Λ_{QCD} . For the tachyon τ , the UV behaviour is constrained by

$$\frac{\tau(z)}{\mathcal{L}} \approx m_q z (-\log \Lambda z)^{-\frac{\gamma_0}{b_0}} + \sigma z^3 (-\log \Lambda z)^{\frac{\gamma_0}{b_0}}, \quad (3)$$

where $\gamma_0 = \frac{3}{2}$, the one-loop coefficient of the anomalous dimension of the mass operator in the dual field theory. Also, \mathcal{L} is the UV AdS radius, i.e., $b(z) \approx \mathcal{L}/z$ as $z \rightarrow 0$, and σ is proportional to the chiral condensate $\langle \bar{q}q \rangle$ with a known proportionality constant [40]. Finally, the boundary value of the scalar potential equals the chemical potential, $\Phi(0) = \mu$, which we set to zero here.

In the far IR, the model is required to lead to confinement. The modelling of the UV and IR behaviors listed above is parametrised in terms of potentials $V_g(\lambda)$, $V_{f_0}(\lambda)$, $\kappa(\lambda)$ and $w(\lambda)$ which appear in the action of the five-dimensional gravity coupled with the scalars discussed above. To determine the high temperature pressure and the vacuum spectrum, we apply the results of [2, 3] with the following set of potentials³:

$$V_g(\lambda) = 12 \left[1 + \frac{88\lambda}{27} + \frac{4619\lambda^2}{729(1+2\lambda)} + 3e^{-1/(2\lambda)}(2\lambda)^{4/3} \sqrt{1 + \log(1+2\lambda)} \right], \quad (4)$$

$$V_{f_0}(\lambda) = W_0 + \frac{8}{27} \left[24 + (11 - 2x_f)W_0 \right] \lambda + \frac{1}{729} \left[24(857 - 46x_f) + (4619 - 1714x_f + 92x_f^2)W_0 \right] \lambda^2 + \frac{120\lambda^3}{(1+2\lambda)^{2/3}}, \quad (5)$$

$$\kappa(\lambda) = \frac{1}{\left(1 + \frac{115-16x_f}{18}\lambda + 20\lambda^2\right)^{2/3}} \sqrt{1 + \frac{1}{200} \log(1 + \lambda^2)}, \quad (6)$$

$$w(\lambda) = \frac{\sqrt{2/3} \mathcal{L}^2}{\left(1 + \frac{115-16x_f}{18}\lambda + 20\lambda^2\right)^{2/3}} \left[1 + \frac{1}{200} \log(1 + \lambda^2) \right]. \quad (7)$$

The $\mathcal{O}(1)$, $\mathcal{O}(\lambda)$ and $\mathcal{O}(\lambda^2)$ terms are tuned so that the solutions lead to QCD beta function and mass anomalous dimension satisfying the standard UV expansions. The asymptotic value

²The constraint is imposed so that the scheme independent two-loop running is reproduced; see [2, 3] for details.

³Notice that the chosen normalization of the potentials also fixes the UV AdS radius through $\mathcal{L}^2 = 12/(12 - xW_0)$.

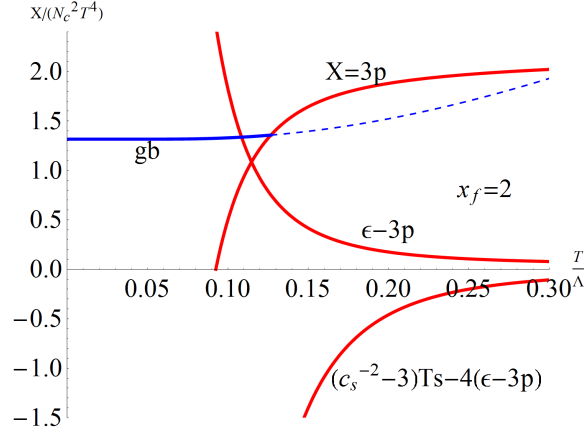


Figure 1: The scaled plasma phase pressure and its first and second $\log T$ -derivatives, plotted for $x_f = 2$ and for small T (for the relations to energy density ϵ and sound velocity c_s^2 , see 21 and 22). The potentials used are those in Eqs.(4)-(6). At $T \rightarrow \infty$ the $3p_q$ curve approaches $3\pi^2/10 = 2.96$ and the zero of the pressure is at $T/\Lambda = 0.0925$. At $T \rightarrow 0$ the Goldstone bosons have $3p_h/(N_c^2 T^4) = x_f^2 \pi^2/30$. Without massive hadrons there would be a 1st order transition at $T = 0.125 \Lambda$. Including the massive hadrons in 10 and 13 gives only a marginal effect in the curve marked gb.

of V_{f0} in the UV, W_0 , remains a parameter. Its range is $0 < W_0 < 12/x_f$ and we have chosen $W_0 = 3/11$.

In the IR, at large λ , confinement (area law) and linearity of the asymptotic glueball trajectories at high excitation numbers require that $V_g \sim \lambda^{4/3} \sqrt{\log \lambda}$ [5]. Moreover we have chosen the remaining parameters in (4) such that a good fit to YM thermodynamics is obtained, and the form of V_{f0} , κ and w at large λ (as well as the value of W_0) such that the phase diagram as a function of x_f is reasonable and the asymptotics of the meson spectra is linear with equal slopes in all sectors [11, 2].

To obtain thermodynamics, one searches for black hole solutions with a horizon at $z = z_h$:

$$f(z_h) = 0, \quad -f'(z_h) = 4\pi T, \quad s = \frac{A}{4G_5} = \frac{b^3(z_h)}{4G_5}. \quad (8)$$

Using the code in [38] thermodynamics can be computed for a given set of model functions. As an example, Fig. 1 shows for $x_f = 2$ the scaled pressure p_q/T^4 and its first and second derivatives with respect to $\log T$. Note that the second derivative is negative. The pressure is Stefan-Boltzmann-normalised, i.e., $p_q/(N_c^2 T^4) \rightarrow (2 + \frac{7}{2} x_f) \pi^2/90$ as $T \rightarrow \infty$. It is this set of curves (and similar ones for $x_f = 1, 2.5$) that we take as the equation of state in the plasma phase.

As discussed in the introduction, this holographic setting, in addition to the thermodynamics, allows also the vacuum spectrum to be determined [11]. The computation involves linearising the equations of motion around the extremal solutions of the action of the model and solving these linearised equations of motion. In this sense it is the 1loop computation discussed in the Introduction. For the potentials of Eqs. (4)-(7), the lowest vector masses

are computed to be

$$2.815, \quad 4.731, \quad 6.076, \quad 7.188, \quad (x_f = 1), \quad (9)$$

$$0.707, \quad 1.156, \quad 1.477, \quad 1.744, \quad (x_f = 2), \quad (10)$$

$$0.0795, \quad 0.1270, \quad 0.1612, \quad 0.1897, \quad (x_f = 2.5), \quad (11)$$

while the lowest scalar masses are

$$2.640, \quad 4.568, \quad 5.857, \quad 6.958, \quad (x_f = 1), \quad (12)$$

$$0.599, \quad 1.102, \quad 1.405, \quad 1.670, \quad (x_f = 2), \quad (13)$$

$$0.06224, \quad 0.1198, \quad 0.1519, \quad 0.1802, \quad (x_f = 2.5), \quad (14)$$

all in units of Λ . The axial vector and pseudoscalar masses are less relevant since they are larger; the lowest axial vector masses are 4.289, 1.092, 0.1249 and the lowest pseudoscalar masses are 4.863, 1.173, 0.1279 for $x_f = 1, 2, 2.5$, respectively. Including these states and their radial recurrences using formulas in the following section gives the pressure marked gb in Fig. 1. In the relevant transition region they have a marginal effect, the temperature in the quark phase is so low that these massive hadronic states are hardly excited.

2.2 The pressure at low temperature modelled as a hadron gas

At $T \rightarrow 0$ the relevant degrees of freedom are the Goldstone bosons spanning the coset space $SU(N_f) \times SU(N_f) / SU(N_f)$. The pressure of these massless bosons is

$$\frac{3p}{N_c^2 T^4} = x_f^2 \frac{\pi^2}{30}, \quad (15)$$

which is also shown in Fig. 1. This contribution alone, when matched with the high temperature contribution determined in the previous section, would lead to strong first order chiral transition at $T = 0.125 \Lambda$ at $x_f = 2$. However, also the massive hadrons are expected to contribute to thermodynamics for temperatures around or higher than their masses. Above we saw that the calculable low-spin masses with their radial excitations have a negligible effect in the T range relevant for phase transitions, a complete mass spectrum, possibly also with mesonic interactions, is needed.

Generally, the ideal boson gas pressure per degree of freedom is

$$p_h(T, \mu, m) = \int \frac{d^3p}{(2\pi)^3} \frac{p^2}{3E} \frac{1}{e^{(E-\mu)/T} - 1} = \frac{T^2 m^2}{2\pi^2} \sum_{k=1}^{\infty} \frac{1}{k^2} e^{k\mu/T} K_2\left(k \frac{m}{T}\right). \quad (16)$$

We will set $\mu = 0$ for the rest of this paper, but we will need formulas with μ to impose interactions via the excluded volume effect (see Eq. (28) below). From here one derives further

$$T \frac{\partial}{\partial T} \frac{p_h(T, m)}{T^4} = \frac{1}{2\pi^2} \sum_{k=1}^{\infty} \frac{1}{k} \frac{m^3}{T^3} K_1\left(k \frac{m}{T}\right), \quad (17)$$

and

$$\left(T \frac{\partial}{\partial T}\right)^2 \frac{p_h(T, m)}{T^4} = \frac{1}{2\pi^2} \sum_{k=1}^{\infty} \left[\frac{m^4}{T^4} K_0\left(k \frac{m}{T}\right) - \frac{2}{k} \frac{m^3}{T^3} K_1\left(k \frac{m}{T}\right) \right]. \quad (18)$$

We want to fold the pressure with the mass spectrum

$$\rho(m, b, a, m_0) = \delta(m) + \frac{\rho_0}{m_0} \left(\frac{m}{m_0}\right)^a e^{bm} \theta(m - m_0), \quad (19)$$

where ρ_0 is a dimensionless number. The degeneracy factor N_f^2 of the $m = 0$ Goldstone bosons and the massive flavor nonsinglet states was factored out from (19). For the massive states with $m > m_0$, we assume an exponential Hagedorn spectrum together with a power of m . Using this spectrum we get for the scaled hadron gas pressure

$$\hat{p}_h(T, b, a, \rho_0, m_0) \equiv \frac{p_h}{N_c^2 T^4} = \frac{\pi^2}{90} x_f^2 + \frac{\rho_0}{m_0} x_f^2 \int_{m_0}^{\infty} dm \frac{m^a}{m_0^a} e^{bm} \frac{m^2}{2\pi^2 T^2} K_2\left(\frac{m}{T}\right), \quad (20)$$

where we approximated⁴ the sum over k by the first term $k = 1$ in the contribution from massive states. Note that the dimensionless quantity p/T^4 can only depend on the dimensionless combinations T/m_0 and bm_0 .

We will aim at matching the 1st and 2nd logarithmic derivatives of the pressure with those of the high temperature phase, so we compute their expressions here. By using (17) and (18) we find that

$$\hat{p}'_h(T, b, a) \equiv T \frac{\partial}{\partial T} \frac{p_h}{N_c^2 T^4} = \frac{\epsilon - 3p}{N_c^2 T^4} = \frac{\rho_0}{m_0} x_f^2 \int_{m_0}^{\infty} dm \frac{m^a}{m_0^a} e^{bm} \frac{m^3}{2\pi^2 T^3} K_1\left(\frac{m}{T}\right) \quad (21)$$

and

$$\begin{aligned} \hat{p}''_h(T, b, a) &\equiv \left(T \frac{\partial}{\partial T}\right)^2 \frac{p_h}{N_c^2 T^4} = \frac{(c_s^{-2} - 3)(\epsilon + p) - 4(\epsilon - 3p)}{N_c^2 T^4} \\ &= \frac{\rho_0}{m_0} x_f^2 \int_{m_0}^{\infty} dm \frac{m^a}{m_0^a} e^{bm} \frac{m^3}{2\pi^2 T^3} \left[\frac{m}{T} K_0\left(\frac{m}{T}\right) - 2K_1\left(\frac{m}{T}\right) \right]. \end{aligned} \quad (22)$$

Note how both of these vanish in the conformal case $\epsilon = 3p$ and $c_s^2 = 1/3$.

So far we have not specified the physical value of the unit of energy Λ . It is the same for thermodynamics (Fig. 1) and the hadron masses (Eqs.(9)-(14)). It could be fixed in GeV units if one, e.g., knew T_c in GeV units for $x_f = 1$. Its x_f dependence requires further study.

The integrals in (20)-(22), of course, blow up for $T > T_{\text{Hagedorn}} = 1/b$. However, exactly at $T = 1/b$ the integrand at large m is $\sim m^{a+3/2+i}$, where i is the order of the derivative, so that the m -integral converges for sufficiently negative a . The hadron gas pressure then does not diverge but approaches a constant as $T \rightarrow 1/b$ from below. This will be the case in practice.

⁴Note that including only the $k = 1$ term provides a very good approximation: even at $m = 0$ the exact result $\hat{p}_h(T, 0) = \pi^2/90 = 0.10966$ deviates just a little from the approximate one $1/\pi^2 = 0.1013$.

To further elaborate on the functional form of the spectral weight $\rho(m)$, we note first that experimental hadron data cannot fix the form of the spectral weight. Simply, the available range of masses is too small to, e.g., separate a power from exponential. For example, over the range $1 < m/\text{GeV} < 2$ numerically [22, 25]

$$4.52 \exp(2.76 m/\text{GeV}) \approx \frac{0.48}{((m/\text{GeV})^2 + 0.25)^{5/2}} \exp(5.75 m/\text{GeV}). \quad (23)$$

We also note that a large number of papers have been written on $\rho(m)$, starting from the classics by Hagedorn [13], Huang-Weinberg [14] and Frautschi [15]. Some examples are as follows: Ref. [16] computes $\rho(m)$ in the bag model, [17] writes “confining phase is consistent with effective string theory in which conformal symmetry and modular invariance play a significant role”, [18] for the first time discusses a separate density for mesons and baryons, but believes that they should be equal to exponential accuracy, [19] tries to connect hadronic and plasma phases like here, [20]-[22] believes that the mesonic and baryonic densities should be different and fits both of them, [24] doubts the empirical validity of the exponential mass spectrum and [25] updates mass spectrum fits and includes the chemical potential in the hadron gas discussion. From all the work on $\rho(m)$ it is obvious that there is no unique parametrisation for it.

3 Connecting hadron gas with plasma

We now keep fixed the plasma phase thermodynamics, plotted in Fig. 1 for $x_f = 2$. The solution is chirally symmetric, i.e., corresponds to the zero value of the bulk tachyon τ . The pressure of the plasma phase vanishes at $T/\Lambda = 0.0925$ for $x_f = 2$. In the hadron phase the pressure is given in (20) and depends on a number of parameters. The question then is how QCD dynamics connects these two curves and what this implies for the properties of the hadron phase.

We shall attempt to make the transition as continuous as possible. For this one needs to satisfy the matching conditions, in increasing order:

- 1st order transition: only \hat{p} continuous,
- 2nd order transition: Both \hat{p} and \hat{p}' continuous,
- 3rd order transition: \hat{p} , \hat{p}' and \hat{p}'' continuous.

To begin with, in the hadronic phase at low T one at least has massless Goldstone bosons, which concretely arise due to chiral symmetry breaking. Their $T \rightarrow 0$ contribution to $3\hat{p}_h$, $x_f^2 \pi^2/30$, is also plotted in Fig. 1, together with a marginal effect of the lowest calculable masses. The curve denoted by “gb” in the figure simply continues to the plasma line and gives a 1st order chiral (and deconfining) transition when one moves from one pressure curve to the other. The transition temperature would be at $T_{\text{gb}} = 0.125 \Lambda$, somewhat higher than 0.0925Λ (where the pressure of the plasma phase goes to zero).

The model formally has 5 parameters: m_0, b, a, ρ_0 and⁵ the value of T_c . The minimum mass m_0 can be determined holographically by a separate computation, see Eqs. (9)-(14). This is conceivably possible also for the Hagedorn temperature $1/b$, but this has not yet been done. Further, a is expected to be negative and T_c has to be somewhat above the point at which p_q vanishes in Fig. 1. Even though the number of parameters is in principle high enough to match all conditions, it is not clear that a solution exists. In fact, we shall see that a third order solution is found only if interactions in the hadron gas are taken into account. This happens à la Van der Waals by including the effects of finite size of hadrons.

Even if we ultimately determine the parameters a, ρ_0 and T_c by numerical fitting, it is useful to have a simple toy model to estimate their values. To obtain the functional form of Eq. (19), consider the eigenvalues N of the operator $\sum_{n=1}^{\infty} \sum_{\mu=1}^{d-2} n N_{\mu n}$. The degeneracy of the eigenvalue is $(d-2)$ (is the number of transverse dimensions) [12]

$$P(N, d) = \frac{1}{\sqrt{2}} \left(\frac{d-2}{24} \right)^{(d-1)/4} N^{-\frac{d+1}{4}} \exp \left(2\pi \sqrt{\frac{d-2}{6}} N \right). \quad (24)$$

We change this to mass density by $P(N, d)dN = \rho(m)dm$, $N = \alpha' m^2$:

$$\rho(m) = \sqrt{2} \sqrt{\alpha'} \left(\frac{d-2}{24} \right)^{\frac{d-1}{4}} (\sqrt{\alpha'} m)^{-\frac{d-1}{2}} \exp \left(2\sqrt{\frac{d-2}{6}} \pi \sqrt{\alpha'} m \right). \quad (25)$$

Choosing $d = 5$ and $m_0 = 1/\sqrt{\alpha'}$ this is of the form (19) with

$$\rho_0 = \frac{\sqrt{2}}{8} \approx 0.177, \quad a = -2, \quad b m_0 = \pi \sqrt{2} \approx 4.44. \quad (26)$$

Our final 3rd order numbers will not agree with this toy model.

3.1 Second order transition

A second order transition, i.e., a transition where \hat{p} and \hat{p}' are continuous, is very easy to obtain. As an example, consider the model (26). Then one has two quantities to determine: the minimum mass m_0 and the transition temperature T_c . One first determines $m_0 = m_0(T)$ numerically by requiring continuity of \hat{p}' . Then inserting this to the continuity condition for \hat{p} , one determines the value⁶ of $T_c = 0.5987$, giving finally $m_0 = m_0(T_c) = 3.158$. The thermodynamics so obtained is plotted in Fig. 2. One observes that the minimum mass obtained from the thermal fit is close to the directly determined one in (9) but somewhat bigger.

To have an idea of the range of acceptable parameter values, take the computed value $m_0 = 2.8$ from (9). Assume a has some fixed value. Then we have 3 parameters to determine, T_c, b, ρ_0 , but only two equations, equality of p/T^4 and its $\log T$ -derivative. By

⁵With the understanding that also the continuity of pressure is a constraint for the parameters. Then also the critical temperature, i.e., the temperature where the constraints are evaluated, is a free parameter.

⁶The numerical values of dimensionful quantities here and below are given in units of Λ , unless stated otherwise.

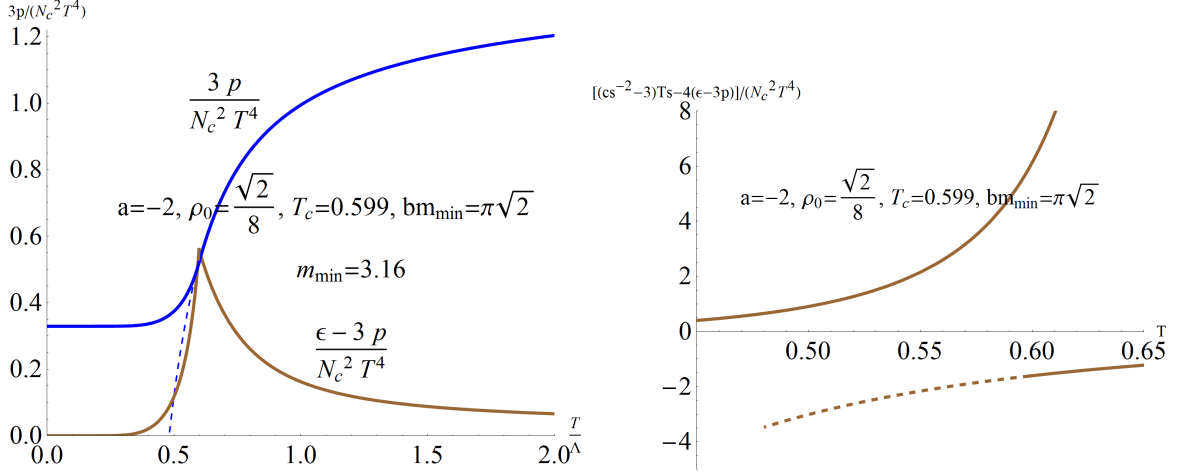


Figure 2: Left: Thermodynamics at $x_f = 1$ with the toy model parameters in (26) and the fitted values $T_c = 0.5987$, $m_0 \equiv m_{\min} = 3.158$. Right: The 2nd derivatives as functions of T . Note the opposite signs, corresponding to the sharp peak in the interaction measure in the left panel.

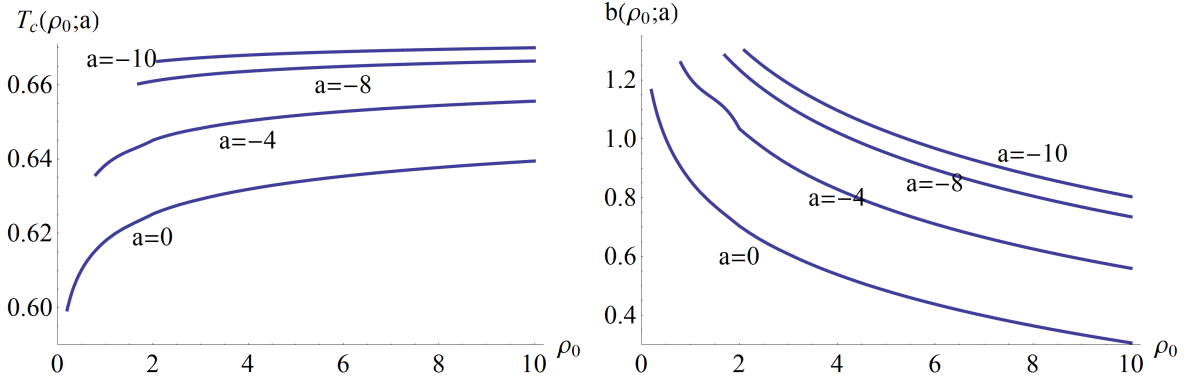


Figure 3: Fitted values of $T_c(\rho_0; a)$ (left) and $b(\rho_0; a)$ (right) for $x_f = 1$ and $m_0 = 2.8$.

demanding that the derivatives coincide one first determines $b = b(T_c, \rho_0)$. The equation $p_h(T_c, b(T_c, \rho_0), \rho_0) = p_q(T_c)$ then gives $T_c = T_c(\rho_0)$ and finally $b = b(T_c(\rho_0), \rho_0) = b(\rho_0)$. The outcomes for T_c and b are plotted in Fig. 3 as functions of the normalisation of mass spectrum ρ_0 and for various fixed values of a .

3.2 Third order transition with pointlike mesons

The next stage is to also require that the 2nd derivatives be equal when we move from p_h to p_q . Since pressure in the plasma phase is taken to be fixed and $\hat{p}_q'' < 0$, one also has to change the sign of \hat{p}_h'' from positive to negative, see the right hand plot in Fig 2. If the second derivatives are equal and negative at some T_c , \hat{p}_h'' must have a zero somewhere. At the same

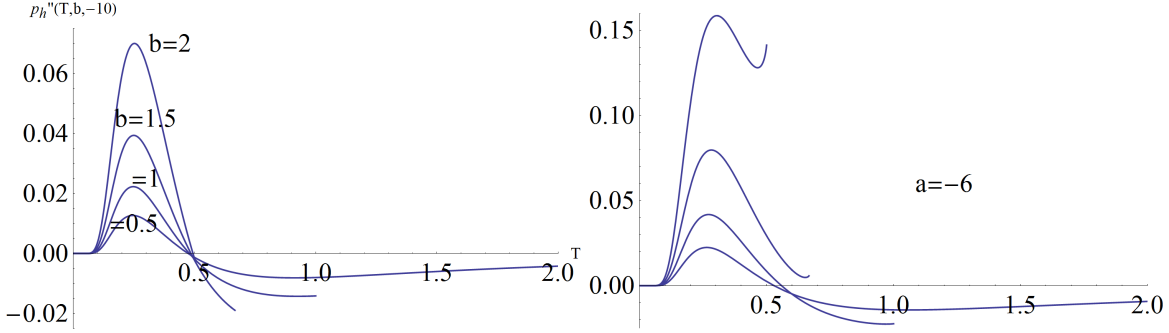


Figure 4: The second derivative in (22) with $m_0 = \rho_0 = x_f = 1$, evaluated for $a = -10$ and $a = -6$ and (curves from bottom) $b = 0.5, 1, 1.5, 2$. For $b \gtrsim 2$ the negative part disappears. The curves end at $T = 1/b$. The zero of $\hat{p}_h''(T, b, a)$, if any, is at $T \approx 0.5$ largely independent of the values of b, a .

point the interaction measure \hat{p}_h' will have an extremum and the sharp peak has disappeared.

To see the sign of $\hat{p}_h''(T, b, a)$ in (22) one can write it in the form

$$\hat{p}_h''(T, b, a) = \frac{\rho_0}{2\pi^2} \frac{T^{a+1}}{m_0^{a+1}} \int_{m_0/T}^{\infty} dy y^{a+3} e^{bTy} y^3 [yK_0(y) - 2K_1(y)]. \quad (27)$$

The sign is determined by the combination $yK_0(y) - 2K_1(y)$ which has a zero at $y = 2.3864$. At small y this combination is negative and behaves approximately as $-2/y - 2y \log(y)$, while at large y it is positive and behaves approximately as $e^{-y} \sqrt{\pi y/2}$. Thus the lower limit m_0/T allows only positive values if $T/m_0 < 1/2.3864 = 0.419$. To have a desired negative value the integral must probe the negative region below $y = 2.3864$ by having $T > 0.419 m_0$. Not much of it is needed as seen from the numerical plots in Fig. 4 (where $m_0 = 1$), $\hat{p}_h''(T, b, a) < 0$ for $T \gtrsim 0.5$ almost independent of the values of b and a . At this temperature then first derivative, i.e., scaled $\epsilon - 3p$ has a maximum and the sharp peak in the interaction measure has disappeared.

For $x_f = 1$ one has $m_0 \approx 2.8$ and one can expect \hat{p}_h'' to become negative only for $T > 0.5 m_0 \approx 1.4$. This would push the maximum of the interaction measure to values of T much larger than those encountered earlier, which are about 0.6. It is physically obvious that the hadron gas phase cannot be thermodynamically stable up to such large T . One concludes that with the present hadron gas model, pointlike hadrons, the sign of \hat{p}_h'' cannot be changed, the cusp in the interaction measure cannot be removed and the transition cannot be made of higher than 2nd order.

4 Third order transition with excluded volume corrections

Let us then check if including hadron interactions via the excluded volume correction [26, 27, 28] would make it possible to make the transition of third order and to get rid of the cusp in the interaction measure. One replaces $V \rightarrow V - v_0 N$ where $v_0 \equiv 1/T_0^3$ is the volume of a single meson and N the number of mesons. What is the new pressure $p(T, \mu)$, given

the pointlike boson pressure $p_0(T, \mu)$ in (16)? Here μ is the chemical potential associated with the meson number N ; i.e. $n = N/V = \partial p / \partial \mu$. The chemical potential associated with conserved baryon number is taken to be zero.

According to a related model in [28] the effective hadron volume is $\frac{16}{3} \pi r_h^3 = (7.93/\text{GeV})^3 = 1/T_0^3$ so that $T_0 = 0.126 \text{ GeV}$. In QCD $T_c \approx 0.15 \text{ GeV}$ while in our units $T_c/\Lambda \approx 0.5$ (where we reinstated the unit of energy Λ). Thus $\Lambda \approx 2T_c \approx 0.3 \text{ GeV}$ so that an expected magnitude at $x_f = 1$ is $T_0/\Lambda \approx 0.42$. We shall find below by matching the pressures of the two phases for $x_f = 1$ that $T_c/T_0 \approx 3$, $T_0/\Lambda \approx 0.25$.

As shown in detail in [27], Section II, $p(T, \mu)$ is obtained⁷ as a solution of the transcendental equation

$$p(T, \mu) = p_0(T, \mu - \frac{1}{T_0^3} p(T, \mu)). \quad (28)$$

Taking the partial derivative with respect to μ of (28) one obtains for the number density

$$n(T, \mu) = \frac{n_0(T, \mu - \frac{1}{T_0^3} p(T, \mu))}{1 + \frac{1}{T_0^3} n_0(T, \mu - \frac{1}{T_0^3} p(T, \mu))}. \quad (29)$$

Thus, to apply this, one has to solve $p(T, \mu)$ from (28).

In the Maxwell-Boltzmann (MB) approximation $e^{\beta(E-\mu)} \gg 1$, and only the $k = 1$ term in the series (16) contributes,

$$p_0(T, \mu) = \frac{m^2 T^2}{2\pi^2} K_2\left(\frac{m}{T}\right) e^{\mu/T} = T n_0(T, \mu). \quad (30)$$

The μ dependence is a simple exponential and (28) becomes

$$\frac{p(T, \mu)}{p_0(T, \mu)} = \exp\left(-\frac{p_0(T, \mu)}{T T_0^3} \frac{p(T, \mu)}{p_0(T, \mu)}\right) = \exp\left(-\frac{n_0(T, \mu)}{T_0^3} \frac{p(T, \mu)}{p_0(T, \mu)}\right). \quad (31)$$

In our case $\mu = 0$, and inserting this in (31) we see that all quantities are just functions of T . The equation is of the general form $q = e^{-aq}$ which is trivial to solve numerically. More formally, the solution is

$$q(a) = \frac{1}{a} W(a) \quad (32)$$

where $W(a)$ is the Lambert's function, ProductLog in Mathematica parlance. At small a

$$q(a) = \frac{1}{a} W(a) = \sum_{k=0}^{\infty} (-1)^k \frac{(k+1)^{k-1}}{k!} a^k = 1 - a + \frac{3}{2} a^2 - \frac{8}{3} a^3 + \dots, \quad (33)$$

and at large a

$$q(a) = \frac{1}{a} W(a) = \frac{1}{a} (\log a - \log \log a + \mathcal{O}(1)). \quad (34)$$

⁷In this section, p_0 is the pressure of pointlike hadron gas, p is the pressure when excluded volume effects are included.

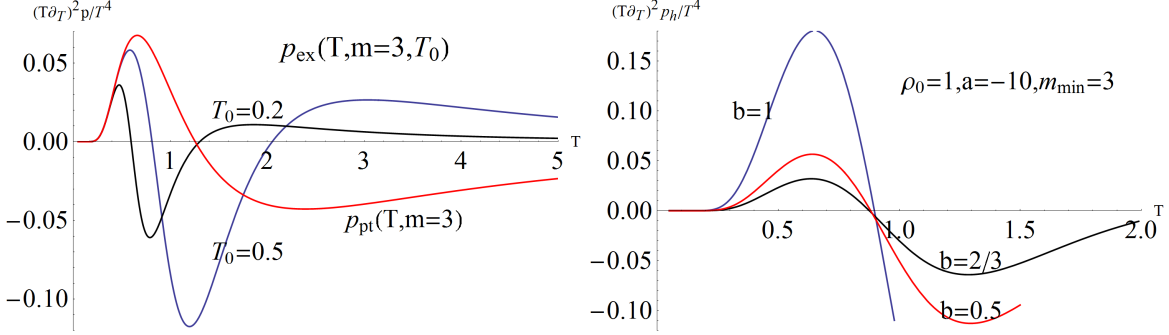


Figure 5: Left: The second derivative $(T\partial_T)^2 p/T^4$ of the excluded volume solution (35) for $m = 3$ and two values of the meson volume parameter T_0 . The pointlike curve (18) (with $k = 1$) is also shown. Right: The $\rho(m)$ -integral of the second derivative of the excluded volume solution (35) of (31) with $\rho_0 = x_f = 1$, $a = -10$, $m_0 \equiv m_{\min} = 3$, $T_0 = 0.5$, and (curves from bottom) $b = 0.5, 2/3, 1$.

Thus the pressure after excluded volume corrections is

$$p(T) \equiv p(T, m, T_0) = T T_0^3 W\left(\frac{p_0(T)}{T T_0^3}\right) = T T_0^3 W\left(\frac{m^2 T}{2\pi^2 T_0^3} K_2\left(\frac{m}{T}\right)\right). \quad (35)$$

At small T/m , $n_0(T) \sim \exp(-m/T)$ is small and

$$p(T) = p_0(T) \left(1 - \frac{n_0(T)}{T_0^3} + \dots\right) \quad (36)$$

and at large T

$$p(T) = T T_0^3 \left(3 \log \frac{T}{T_0} - \log \log \frac{T}{T_0} + \mathcal{O}(1)\right). \quad (37)$$

It is also illuminating to evaluate the effect of volume exclusion on the number density at large T . In (29) there is an additional suppression factor $\exp(-p/(T T_0^3)) = \mathcal{O}(1) T_0^3 / T^3$, where we used (31) and (37) to obtain the estimate. Therefore the excluded volume density at large T is simply $n = \mathcal{O}(1) T_0^3$, the hadrons are densely packed but do not overlap. Related to this, in the excluded volume model the effective chemical potential $-p(T, 0)/T_0^3$ is always negative and one does not get to the Bose-Einstein condensation domain $\mu \rightarrow m$ where meson wave functions overlap.

As a first step towards understanding the effects of excluded volume, the left panel of Fig. 5 shows numerical results for the 2nd log T derivative of the scaled pressure solution (35) of (28) for $m = 3$. There the red curve corresponds to the pointlike pressure, the $k = 1$ term in (18). As discussed above, the 2nd derivative is negative for $T > m/2.386 = 1.257$. The two excluded volume curves correspond to meson volume parameter values $T_0 = 0.2$ and 0.5 . Here 0.5 is chosen so that the hadron volume is of the order of $1/T_c^3$ with T_c as in previous figures. The small T behavior is always like in the pointlike case, the large T behavior shows the positive 2nd derivative following from (37) and in between there is a negative

region. Increasing T_0 would extend the negative region to the right so that it asymptotically approaches the pointlike curve. In any case meson finite size enhances the negative region.

As a second step, the right panel of Fig. 5 shows numerical results for the 2nd log T derivative of the scaled pressure solution (35) of (28) at $T_0 = 0.5$ but now integrated over the exponential mass spectrum (19) $\rho(m, b, a, m_0)$. A large negative value of a is needed, here $a = -10$. Since we have an exponential mass spectrum, the computation can only be valid up to $T = 1/b$. Since plasma extends down to $T = 0.5$, we certainly must have $b < 2$.

Comparing with Fig. 4 one sees that indeed excluded volume based interactions increase the magnitude of the negative 2nd derivative even when integrated over exponential mass spectrum. The parameter ρ_0 can be used to increase the magnitude further.

Above in (30) we used the Maxwell-Boltzmann approximation which, due to its explicit μ dependence, led to simplified computations. Without invoking the MB approximation, instead of $q = e^{-aq}$, one has to solve the equation

$$q = \frac{\sum_1^\infty \frac{1}{k^2} e^{-kaq} K_2(k \frac{m}{T})}{\sum_1^\infty \frac{1}{k^2} K_2(k \frac{m}{T})} \quad (38)$$

for $q = q(a, m/T)$. One can numerically check that this improvement has only a marginal effect. The physics reason for this is that, as discussed above, in the excluded volume model the meson wave packets are densely packed but do not overlap, and one is never close to Bose-Einstein condensation.

Another calculable interaction term is that among Goldstone bosons. Including terms of order 2 and 4 in the chiral Lagrangian and to 3 loops [39, 23] one has

$$p_{\text{gb}}(T) = N_f^2 \frac{\pi^2}{90} T^4 \left(1 + \frac{N_f^2 T^4}{144 f_\pi^4} \log \frac{\Lambda_p}{T} + \mathcal{O}(T^6) \right), \quad (39)$$

where the scale Λ_p depends on the higher order couplings of the bosons. For the interaction measure we find

$$\frac{\epsilon_{\text{gb}} - 3p_{\text{gb}}}{N_c^2 T^4} = \frac{\pi^2}{30} x_f^2 \frac{N_f^2 T^4}{108 f_\pi^4} \left(\log \frac{\Lambda_p}{T} - \frac{1}{4} \right). \quad (40)$$

In the Gell-Mann-Oakes-Renner relation (for a theory with all quark masses equal) $m_\pi^2 f_\pi^2 = -\frac{2}{N_f} m_q \langle \bar{q}q \rangle$ one has $\langle \bar{q}q \rangle \sim N_f N_c$ so that f_π scales as $f_\pi^2 \sim N_c$. Thus in the interaction measure above $N_f^2/f_\pi^4 \sim x_f^2$ and it seems that this term will be dominated by effects from the massive states. As a side remark, it is also repulsive for $T \lesssim \Lambda_p$, it increases p_{gb} there.

5 Fit of parameters and their x_f dependence

We shall now analyse the QCD equation of state (EoS) at $x_f = 1, 2, 2.5$ by requiring continuity of the logarithmic derivatives $(T\partial/\partial T)^n(p/T^4)$, with $n = 0, 1, 2$. We use p_q computed from holography and the hadronic phase EoS

$$\hat{p}_h(T, b, a, \rho_0, m_0) \equiv \frac{p_h}{N_c^2 T^4} = \frac{\pi^2}{90} x_f^2 + \frac{\rho_0}{m_0} x_f^2 \int_{m_0}^\infty dm \frac{m^a}{m_0^a} e^{bm} \frac{T_0^3}{T^3} W \left(\frac{m^2 T}{2\pi^2 T_0^3} K_2 \left(\frac{m}{T} \right) \right), \quad (41)$$

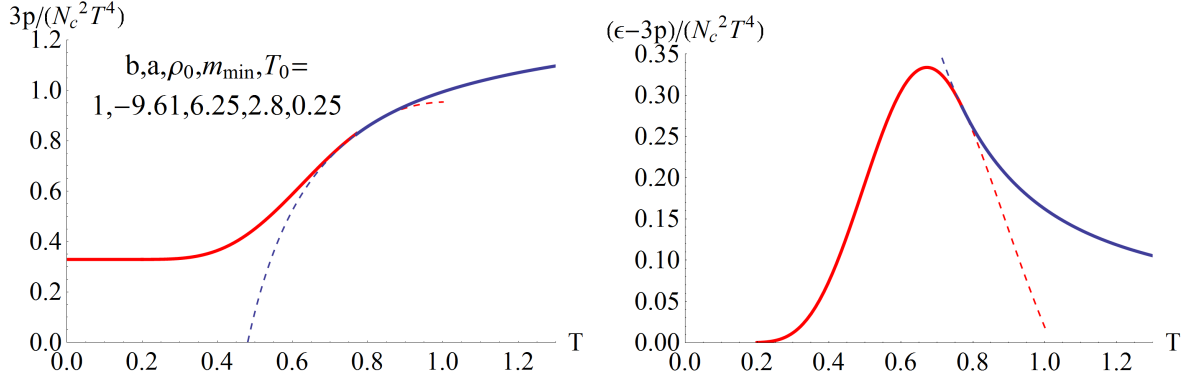


Figure 6: Pressure and interaction measure with a 3rd order phase transition at $x_f = 1$, i.e., with $N_f^2 = N_c^2$ massless Goldstone bosons. Stable phases are continuous, metastable ones dashed. The maximum of interaction measure is at $T = 0.672$ in the hadron gas phase, hadron gas is the stable phase for $T < 0.771$ and ends at $T = 1.0$.

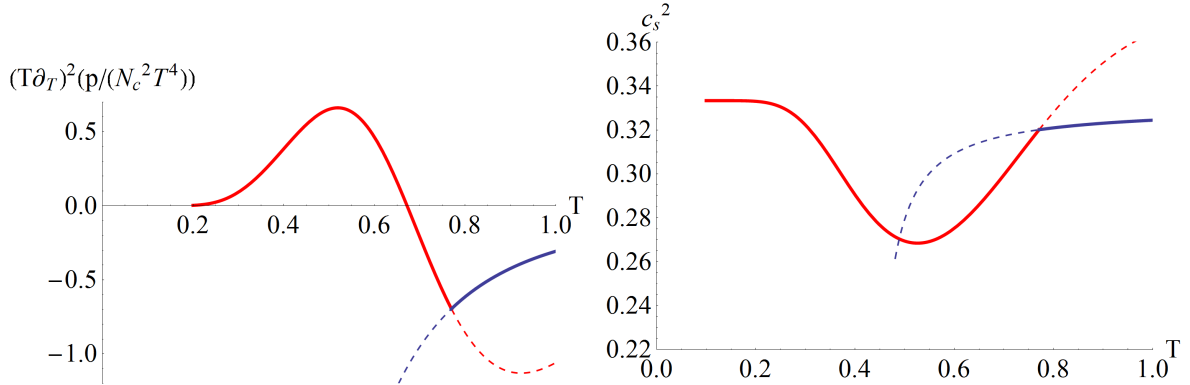


Figure 7: Second $\log T$ derivative of p/T^4 and the sound velocity squared with a 3rd order phase transition at $x_f = 1$. One sees concretely how the 2nd derivative is continuous at $T_c = 0.771$ but the third derivative jumps. The sound velocity squared is continuous at T_c but not its derivative.

where $W(a)$ is as discussed above in (32). The first and second $\log T$ derivatives can be computed analytically but lead to lengthy expressions.

Of particular interest is to see what happens at larger x_f , for values approaching the lower limit of the conformal region. The naive argument comparing the number of degrees of freedom in the conformal limits at $T = 0$ and $T = \infty$ gives the estimate $x_c = 4$. The precise value for the potentials of the bulk action used here can be obtained numerically as explained in [1] and is $x_c = 3.187$. The value 2.5 is already rather close to this, but not yet in the Miransky scaling region $x_c - x_f \ll 1$, where the bound state masses and critical temperatures are expected to decrease as $\sim \exp(-\text{const}/\sqrt{x_c - x_f})$.

The outcome of a numerical application of the excluded volume model for $x_f = 1$ is shown in Figs. 6 and 7. One plots \hat{p} , its first and second derivatives and the sound velocity, related

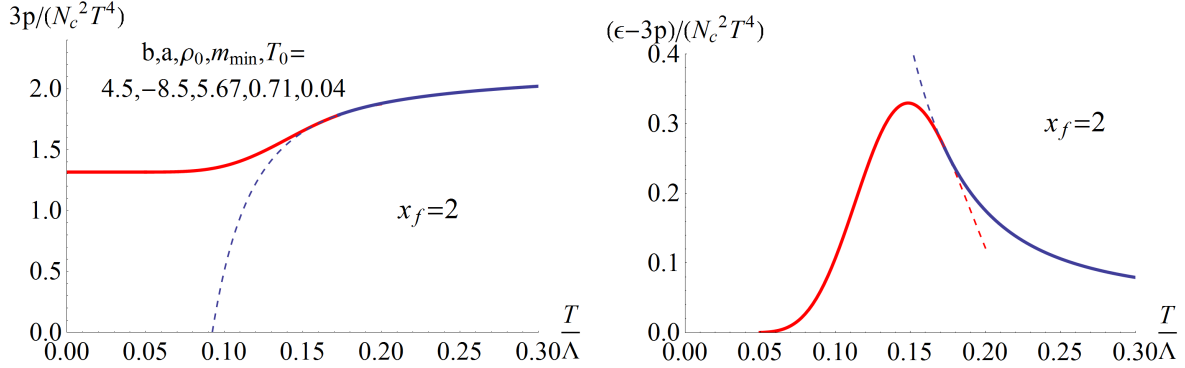


Figure 8: As Fig. 6 but for $x_f = 2$. Hadron gas ends at $T = 0.22$, is the stable phase for $T < 0.173$, the maximum of interaction measure is at $T = 0.147$. Note that if we fix the critical temperature to the QCD value $T_c \approx 0.15$ GeV, we have here $\Lambda \approx 1$ GeV, i.e., the numerical values for the temperatures are close to their physical values measured in units of GeV.

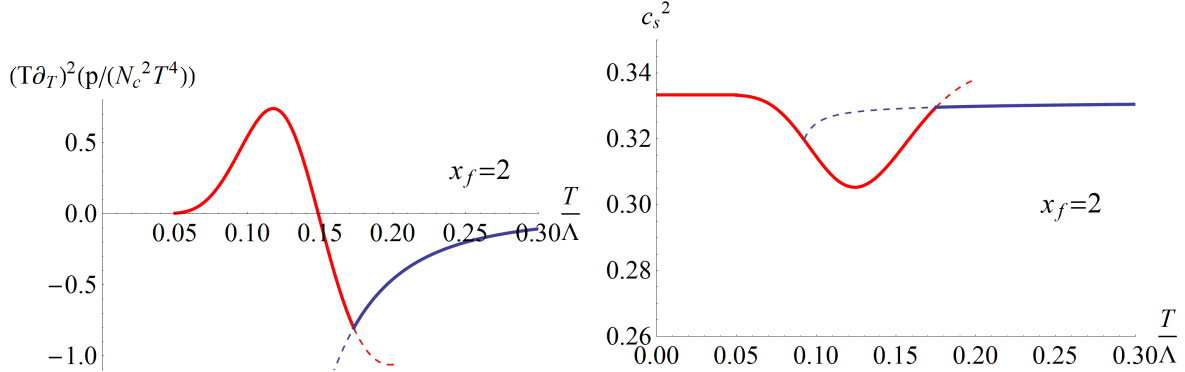


Figure 9: As Fig. 7 but for $x_f = 2$. The 2nd derivative is continuous at $T_c = 0.173$ but the third derivative jumps. The sound velocity squared is continuous at T_c but its derivative has a discontinuity.

to the second derivative as in Eq. (22). Thus indeed a connection between hadron gas in the plasma phase with a third order transition can be established. Not surprisingly, for a wide range of T , $0.7 \lesssim T \lesssim 0.9$, the pressures of the hadron and plasma phases are very close to each other. The role of the repulsive interactions in the hadron gas phase was to bend down the 2nd derivative to negative values. It vanishes when the interaction measure has a maximum. The sound velocity approaches the conformal limit $1/\sqrt{3}$ both when $T \rightarrow 0$ and $T \rightarrow \infty$. With broken chiral symmetry and massive Goldstone bosons, $c_s \rightarrow 0$ at $T \rightarrow 0$.

The outcome at $x_f = 2$ is shown in Figs. 8 and 9 and that for $x_f = 2.5$ in Fig. 10 (where only p and the sound velocity are plotted, 1st and 2nd derivatives are qualitatively as in Figs. 8 and 9). The fit parameters with mass dimension are summarised in Table 1. Here $m_0 \equiv m_{\min}$ is the smallest vector mass, $T(p_q = 0)$ is the temperature at which the plasma pressure vanishes (this is the transition temperature for pure Yang-Mills theory), $T(p_q = p_{\text{gb}})$

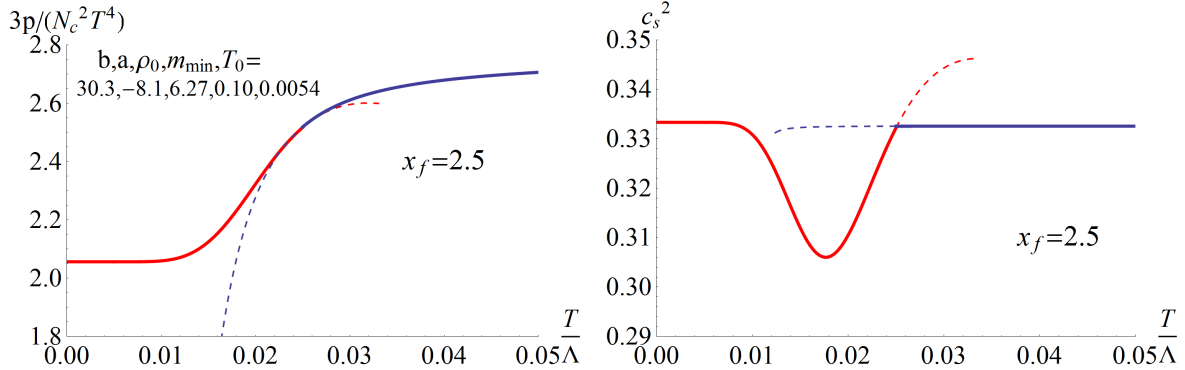


Figure 10: Left: Fit with a 3rd order phase transition for $x_f = 2.5$: the 2nd derivative of p is continuous at $T_c = 0.025$ but the third derivative jumps. The maximum of the interaction measure (not shown) is at $T_{\max} = 0.0209$. Right: The sound velocity squared. It is continuous at T_c but not its derivative.

is the temperature at which the plasma pressure is $p_{\text{gb}} = N_f^2 \pi^2 T^4 / 90$, at T_{\max} the interaction measure has a maximum, at T_c chiral symmetry is restored (the plasma phase becomes the stable phase), T_0 is the meson volume parameter ($v_0 \equiv 1/T_0^3$) and $1/b$ is the Hagedorn temperature (the metastable hadron gas phase ends there).

Although m_0 varies by more than a factor 35, the expectation that parameters with mass dimension scale with m_0 is born out to a 10% accuracy. An exception is the meson size parameter T_0 which decreases by more than expected by mass scaling. Comparing with T_c we have $T_c/T_0 = 3.1, 4.3, 4.6$ for $x_f = 1, 2, 2.5$, respectively. One may note that even at $x_f = 1$ the value of $T_0 = 0.25$ was smaller than the expected value 0.42. Thus with increasing x_f the mesons have to appear effectively larger, the interactions stronger, to bend the hadron gas EoS nearly continuously to the plasma one.

The numerical value of the mass exponent in $\rho(m) \sim e^{bm}$ can be understood by noting that physically the hadron gas as a metastable phase cannot be expected to extend far into the plasma phase. The end point is the Hagedorn temperature $T_H = 1/b$ so that $1/b \gtrsim T_c \approx 0.3m_0$, in agreement with the observation $bm_0 \approx 3$.

The dimensionless parameters vary on a similar level: $(a, \rho_0) = (-9.61, 6.25)$ for $x_f = 1$ is changed to $(-8.5, 5.67)$ for $x_f = 2$ and to $(-8.1, 6.27)$ for $x_f = 2.5$. It is not excluded that constant x_f independent values could be found for these. Anyway it seems that the exponent of the powerlike mass dependence is stably close to -8 and the weight of the massive part of the mass spectrum is about 6.

Note the small range of variation in c_s^2 , which gets monotonically smaller when x_f increases: one is approaching the conformal region where everywhere $c_s = 1/\sqrt{3}$.

One may convert the above temperatures to GeV units by, for example, demanding that $T_c(x_f = 1) = 0.15$ GeV and by assuming that Λ is independent of x_f . Then $\Lambda = 0.194$ GeV and $T_c = 150, 34, 4.9$ MeV at $x_f = 1, 2, 2.5$, respectively. For the determination of scales at large N_f and estimates of the N_f dependence of the critical temperature by using other methods, see, for example, [41, 42, 43].

x_f	m_0	$T(p_q = 0)$	$T(p_q = p_{gb})$	T_{\max}	T_c	T_0	b
1	2.82	0.480	0.542	0.672	0.771	0.25	1
2	0.707	0.0925	0.125	0.147	0.173	0.04	4.5
2.5	0.0795	0.0124	0.0179	0.0209	0.025	0.0054	30.3

x_f	m_0	$\hat{T}(p_q = 0)$	$\hat{T}(p_q = p_{gb})$	\hat{T}_{\max}	\hat{T}_c	\hat{T}_0	bm_0
1	2.82	0.170	0.194	0.238	0.273	0.0887	2.8
2	0.707	0.131	0.177	0.208	0.244	0.0566	3.2
2.5	0.0795	0.156	0.225	0.263	0.314	0.0679	3.0

Table 1: Top: Dependence of mass scales on x_f . Here m_0 is the minimum vector mass. All quantities are in units of Λ . Bottom: Dependence of mass scales on x_f if scaled with m_0 : $\hat{T} \equiv T/m_0$.

6 Second order transition with massive Goldstone bosons

If quark masses are non-zero, they break explicitly chiral symmetry and Goldstone bosons are massive. The hadronic pressure will then vanish at $T = 0$. To see what this implies quantitatively, take the hadron mass spectrum in (19), use the toy model parameters in (26) and replace $\delta(m) \rightarrow \delta(m - m_{gb})$ with $m_{gb} = 0.5 \approx T_c$. The argument here is that for physical QCD T_c is close to m_π . Also the holographic plasma part will, in principle, change; there are only tachyonic chiral symmetry breaking solutions even though the quark mass is very small. We do not yet have these solutions available and stick to the $m_q = 0$ plasma curves. The thermodynamics computed with these assumptions is shown in Fig. 11.

At small T the effect, of course, is striking. One observes further that the minimum mass obtained from thermodynamics is now almost equal to the one from direct computation in (19) and that T_c is only 10% above the temperature at which $p = 0$. Due to this closeness the derivatives are also larger and the peak in interaction measure even sharper.

7 Conclusions

We have in this paper shown concretely how a high T , $\mu = 0$, QCD plasma equation of state, computed from holography at vanishing quark mass, can be connected with a low T hadron gas phase with N_f^2 Goldstone bosons and massive mesons obeying a Hagedorn spectrum with a minimum mass. In the language of holography, the leading holographic computation has been improved by quantum loop and stringy corrections. The holographic computation implies that there is a minimum temperature for the plasma phase and, accordingly, a phase transition is needed. It is very simple to connect the phases with a first or second order transition, and we have shown how a more continuous third order transition can be achieved. The motivation for this is that for physical non-zero quark masses lattice Monte Carlo results suggest that the transition is continuous.

Quantitatively a determining role in the hadron gas phase is played by the minimum mass of the hadrons (mesons in our case). We emphasize that here these minimum masses have

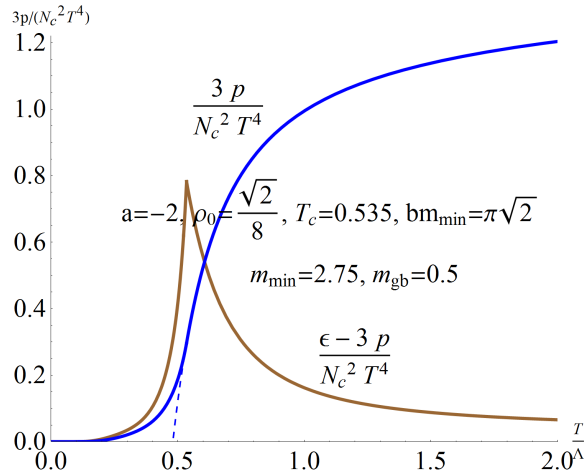


Figure 11: Left: Thermodynamics with toy model parameters in (26) but with massive Goldstone bosons, $m_{\text{gb}} = 0.5 \approx T_c$. The fitted values are $T_c = 0.5348$, $m_0 = 2.754$.

also been computed from the same holographic model at $T = 0$ and at various values of $x_f = N_f/N_c$. The entire spectrum obviously cannot be computed. We have seen here how it and its interactions are constrained by the requirement of as continuous a transition as possible.

An outcome of the computations here is that the thermal parameters with mass dimension scale with the minimum mass when x_f is varied. This is expected to also be true in the Miransky scaling region, i.e., very close to the start of the conformal region at $x_f = x_c \approx 4$.

Our computation, of course, does not prove that the transition is of third order, it just indicates what phenomena are encountered if this is the case. Conceivably one could also impose continuity of the third derivative. Completely analytic expression [28] would, however, require that the plasma EoS extend to $T = 0$ and the hadron gas one to $T = \infty$, which is not possible in our model.

Ultimately, of course, these theoretical ideas should be tested by numerical lattice Monte Carlo simulations, say, at $N_c = 3$ and $N_f = 3, 6, 9, \dots$ as approximations to $N_c, N_f \rightarrow \infty$. Much work has been devoted to this at $T = 0$. The figures above should give a good idea of what can be expected to happen to thermodynamics when x_f is increased. The overriding difficulty is the imposition of vanishing or small quark mass. This holographic computation can also be extended to non-zero μ .

Acknowledgements. We thank J. Kapusta for discussions. This work was supported in part by European Union’s Seventh Framework Programme under grant agreements (FP7-REGPOT-2012-2013-1) No 316165, PIF-GA-2011-300984, the ERC Advanced Grant BSMOX-FORD 228169, and the EU program Thales MIS 375734. It was also co-financed by the European Union (European Social Fund, ESF) and Greek national funds through the Operational Program “Education and Lifelong Learning” of the National Strategic Reference Framework

(NSRF) under “Funding of proposals that have received a positive evaluation in the 3rd and 4th Call of ERC Grant Schemes”, as well as under the action “ARISTEIA”. The research of T.A. is supported in part by Icelandic Research Fund grant 130131-052 and by a grant from the University of Iceland Research Fund.

References

- [1] M. Järvinen and E. Kiritsis, “Holographic Models for QCD in the Veneziano Limit,” *JHEP* **1203** (2012) 002 [arXiv: 1112.1261[hep-ph]].
- [2] T. Alho, M. Järvinen, K. Kajantie, E. Kiritsis and K. Tuominen, “On finite-temperature holographic QCD in the Veneziano limit,” *JHEP* **1301**, 093 (2013) [arXiv:1210.4516 [hep-ph]].
- [3] T. Alho, M. Järvinen, K. Kajantie, E. Kiritsis, C. Rosen and K. Tuominen, “A holographic model for QCD in the Veneziano limit at finite temperature and density,” *JHEP* **1404**, 124 (2014) [arXiv:1312.5199 [hep-ph]].
- [4] I. Iatrakis and I. Zahed, “Spectral Functions in V-QCD with Matter: Masses, Susceptibilities, Diffusion and Conductivity,” arXiv:1410.8540 [hep-th].
- [5] U. Gursoy and E. Kiritsis, “Exploring improved holographic theories for QCD: Part I,” *JHEP* **0802** (2008) 032 [arXiv:0707.1324 [hep-th]];
U. Gursoy, E. Kiritsis and F. Nitti, “Exploring improved holographic theories for QCD: Part II,” *JHEP* **0802**, 019 (2008) [arXiv:0707.1349 [hep-th]].
- [6] R. Casero, E. Kiritsis and A. Paredes, “Chiral symmetry breaking as open string tachyon condensation,” *Nucl. Phys. B* **787** (2007) 98 [hep-th/0702155].
- [7] A. Mocsy, F. Sannino and K. Tuominen, “Confinement versus chiral symmetry,” *Phys. Rev. Lett.* **92**, 182302 (2004) [hep-ph/0308135].
- [8] T. Kahara and K. Tuominen, “Degrees of freedom and the phase transitions of two flavor QCD,” *Phys. Rev. D* **78**, 034015 (2008) [arXiv:0803.2598 [hep-ph]].
- [9] K. Fukushima, “Phase diagrams in the three-flavor Nambu-Jona-Lasinio model with the Polyakov loop,” *Phys. Rev. D* **77**, 114028 (2008) [Erratum-ibid. *D* **78**, 039902 (2008)] [arXiv:0803.3318 [hep-ph]].
- [10] D. Arean, I. Iatrakis, M. Järvinen and E. Kiritsis, “V-QCD: Spectra, the dilaton and the S-parameter,” *Phys. Lett. B* **720**, 219 (2013) [arXiv:1211.6125 [hep-ph]].
- [11] D. Arean, I. Iatrakis, M. Järvinen, E. Kiritsis, “The discontinuities of conformal transitions and mass spectra of V-QCD,” *JHEP* **1311**, 068 (2013) [arXiv:1309.2286 [hep-ph]].
- [12] E. Kiritsis, “String theory in a nutshell,” Princeton University Press, 2007.

- [13] R. Hagedorn, “Statistical thermodynamics of strong interactions at high-energies,” *Nuovo Cim. Suppl.* **3**, 147 (1965).
- [14] K. Huang and S. Weinberg, “Ultimate temperature and the early universe,” *Phys. Rev. Lett.* **25**, 895 (1970).
- [15] S. C. Frautschi, “Statistical bootstrap model of hadrons,” *Phys. Rev. D* **3**, 2821 (1971).
- [16] J. I. Kapusta, “Asymptotic Mass Spectrum and Thermodynamics of the Abelian Bag Model,” *Phys. Rev. D* **23**, 2444 (1981).
- [17] K. R. Dienes and J. R. Cudell, “Conformal invariance and degrees of freedom in the QCD string,” *Phys. Rev. Lett.* **72**, 187 (1994) [hep-th/9309126].
- [18] P. G. O. Freund and J. L. Rosner, “The Densities of meson and baryon states,” *Phys. Rev. Lett.* **68**, 765 (1992).
- [19] A. V. Leonidov and G. M. Zinovev, “On the deconfinement phase transition in the resonance gas,” *JETP Lett.* **63**, 510 (1996) [hep-ph/9408264].
- [20] W. Broniowski, “Distinct Hagedorn temperatures from particle spectra: A Higher one for mesons, a lower one for baryons,” hep-ph/0008112.
- [21] W. Broniowski and W. Florkowski, “Different Hagedorn temperatures for mesons and baryons from experimental mass spectra, compound hadrons, and combinatorial saturation,” *Phys. Lett. B* **490**, 223 (2000) [hep-ph/0004104].
- [22] W. Broniowski, W. Florkowski and L. Y. Glozman, “Update of the Hagedorn mass spectrum,” *Phys. Rev. D* **70**, 117503 (2004) [hep-ph/0407290].
- [23] D. Fernandez-Fraile and A. Gomez Nicola, “Transport coefficients and resonances for a meson gas in Chiral Perturbation Theory,” *Eur. Phys. J. C* **62**, 37 (2009) [arXiv:0902.4829 [hep-ph]].
- [24] T. D. Cohen and V. Krejcirik, “Does the Empirical Meson Spectrum Support the Hagedorn Conjecture?,” *J. Phys. G* **39**, 055001 (2012) [arXiv:1107.2130 [hep-ph]].
- [25] J. Cleymans and D. Worku, “The Hagedorn temperature Revisited,” *Mod. Phys. Lett. A* **26**, 1197 (2011) [arXiv:1103.1463 [hep-ph]].
- [26] J. I. Kapusta and K. A. Olive, “Thermodynamics of Hadrons: Delimiting the Temperature,” *Nucl. Phys. A* **408**, 478 (1983).
- [27] G. D. Yen, M. I. Gorenstein, W. Greiner and S. N. Yang, “Excluded volume hadron gas model for particle number ratios in A+A collisions,” *Phys. Rev. C* **56**, 2210 (1997) [nucl-th/9711062].
- [28] M. Albright, J. Kapusta and C. Young, “Matching Excluded Volume Hadron Resonance Gas Models and Perturbative QCD to Lattice Calculations,” *Phys. Rev. C* **90**, 024915 (2014) [arXiv:1404.7540 [nucl-th]].

- [29] A. Bazavov, H.-T. Ding, P. Hegde, O. Kaczmarek, F. Karsch, E. Laermann, Y. Maezawa and S. Mukherjee *et al.*, “Additional Strange Hadrons from QCD Thermodynamics and Strangeness Freezeout in Heavy Ion Collisions,” *Phys. Rev. Lett.* **113**, no. 7, 072001 (2014) [arXiv:1404.6511 [hep-lat]].
- [30] V. Vovchenko, D. V. Anichishkin and M. I. Gorenstein, “Hadron Resonance Gas Equation of State from Lattice QCD,” arXiv:1412.5478 [nucl-th].
- [31] D. J. Gross and E. Witten, “Possible Third Order Phase Transition in the Large N Lattice Gauge Theory,” *Phys. Rev. D* **21**, 446 (1980).
- [32] S. R. Wadia, “ $N = \infty$ Phase Transition in a Class of Exactly Soluble Model Lattice Gauge Theories,” *Phys. Lett. B* **93**, 403 (1980).
- [33] C. A. Tracy and H. Widom, “Level-spacing distributions and the Airy kernel,” *Comm. Math. Phys.* 159, 151 (1994).
- [34] Celine Nadal and Satya N. Majumdar, “A simple derivation of the Tracy-Widom distribution of the maximal eigenvalue of a Gaussian unitary random matrix,” *Journal of Statistical Mechanics* (2011) P04001.
- [35] R. D. Pisarski and F. Wilczek, “Remarks on the Chiral Phase Transition in Chromodynamics,” *Phys. Rev. D* **29**, 338 (1984).
- [36] T. J. Hollowood and J. C. Myers, “Deconfinement transitions of large N QCD with chemical potential at weak and strong coupling,” *JHEP* **1210**, 067 (2012) [arXiv:1207.4605 [hep-th]].
- [37] T. J. Hollowood, S. P. Kumar and J. C. Myers, “Weak coupling large-N transitions at finite baryon density,” *JHEP* **1111**, 138 (2011) [arXiv:1110.0696 [hep-th]].
- [38] T. Alho, <https://github.com/timoalho/VQCDThermo>.
- [39] P. Gerber and H. Leutwyler, “Hadrons Below the Chiral Phase Transition,” *Nucl. Phys. B* **321**, 387 (1989).
- [40] M. Järvinen, “Massive holographic QCD in the Veneziano limit,” to be published.
- [41] M. Järvinen and F. Sannino, “Extreme Technicolor and The Walking Critical Temperature,” *JHEP* **1102**, 081 (2011) [arXiv:1009.5380 [hep-ph]].
- [42] J. Braun, C. S. Fischer and H. Gies, “Beyond Miransky Scaling,” *Phys. Rev. D* **84**, 034045 (2011) [arXiv:1012.4279 [hep-ph]].
- [43] M. P. Lombardo, K. Miura, T. J. Nunes da Silva and E. Pallante, “One, two, zero: Scales of strong interactions,” *Int. J. Mod. Phys. A* **29**, no. 25, 1445007 (2014) [arXiv:1410.2036 [hep-lat]].
- [44] D. B. Kaplan, J. W. Lee, D. T. Son and M. A. Stephanov, “Conformality Lost,” *Phys. Rev. D* **80** (2009) 125005 [arXiv:0905.4752 [hep-th]].